

# Quasiperiodic Cartwheel Algorithm for $HB$ Tiling Design

Uli Gaenshirt<sup>1</sup> and Amrita Acharyya<sup>2</sup>

<sup>1</sup>Sculptor & Researcher, Nuremberg, Germany; uli.gaenshirt@gmail.com

<sup>2</sup>Department of Mathematics and Statistics, University of Toledo, Ohio 43606, USA; amrita.acharyya@utoledo.edu

## Abstract

In this paper, we propose an algorithm for creating figurative quasiperiodic tilings by duplicating individually drawn lines and assembling them according to the order of a quasiperiodic  $HB$  cartwheel. The Penrose  $HB$  tiling, first introduced in 2015 by one of us (*Uli*), is a variant of the Penrose rhombus tiling. The transformations of the two prototiles, elongated hexagonal tiles  $H$  and paper boat-shaped tiles  $B$ , are expressed as complex equations. We use representative examples for each step. The equations are illustrated by geometric and figurative images. Our goal is to work with computer scientists to develop a computer program based on the proposed algorithm. This would enable users to engage in an artistic design process. The program would visualize the edges drawn by the users in a large quasiperiodic  $HB$  cartwheel arrangement.

## Introduction

In terms of the *quasiperiodic Penrose tiles* as decorated puzzle pieces, the largely unknown *Penrose  $HB$  tiling* ( $H$  stands for *hexagon* and  $B$  for *boat*) offers advantages over the well-known Penrose tilings P1, P2 and P3 [9][2], as its geometric prototiles have no acute  $36^\circ$  angles like these. The angles of the  $HB$  tiles are always multiples of  $72^\circ$ . The mirrored  $H^*$  and  $B^*$  tiles, which are required in the  $HB$  tiling, give the design a sense of balance. In 2025, we have already proposed some mirrored tiles in [2] using the kite and dart tiling P2, the Penrose rhombus tiling P3 and the  $HB$  tiling.

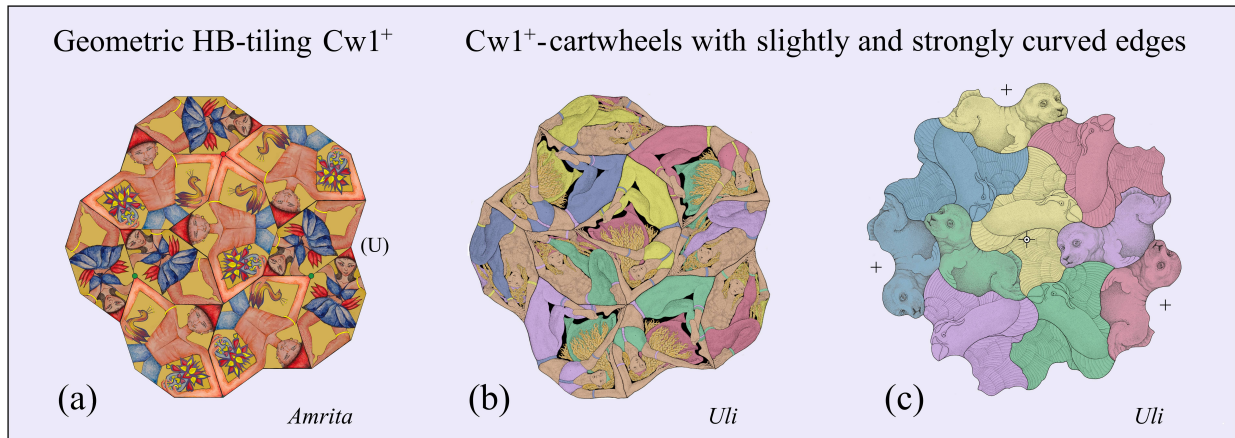


**Figure 1:** Cartwheels  $Cw1^+$ : (a) Circus artists. (b) Ballet dancers. (c) Birds and baby seals.

The geometric  $HB$  cartwheel  $Cw1^+$  in Figure 1(a) is an arrangement of three  $B$  tiles, two  $B^*$  tiles, four  $H$  tiles, and one  $H^*$  tile. It has an asymmetrical center but an outline with *fivefold rotational symmetry*. When generating larger cartwheels [4], the numbers of the five different tile orientations become more and more similar. The result is a *structural, fivefold rotational symmetry* that cannot be *periodical*! The *curved edges* [5][6] in Figure 1(b) and 1(c) represent the *matching rules*, which prevent periodicity and enforce a *quasiperiodic (almost periodic) order*, even when the tiles are freely arranged. For the geometric  $HB$  tiles in Figure 1(a), the structural fivefold symmetry can only be achieved by marking the edges.

## Matching Rules of Geometric *HB* Tilings Enforced by Triple Arrows

The geometric *HB* tiles in Figure 2(a) are provided with edge marks that represent the matching rules and create a quasiperiodic order with a structural fivefold rotational symmetry. We here propose *triple arrows*, which consist of three triangles arranged in a row. In the vertical *B* tile orientation, the triangle arrows always point upwards from the apex *V* to the top point *T*. For an edge *a*, the back triangle is black, for an edge *b*, the middle triangle is black, and for an edge *c*, the front triangle is black. At the “mirrored” edges *a\**, *b\** and *c\**, the black triangles turn white and the white triangles turn black. Only edge types in Figure 2(c) have true mirror images. The arrows at the points *T* indicate the orientation of the tiles. In globally designed arrangements, the *B* tiles are the controlled tiles, while the *H* tiles merely fill the gaps.

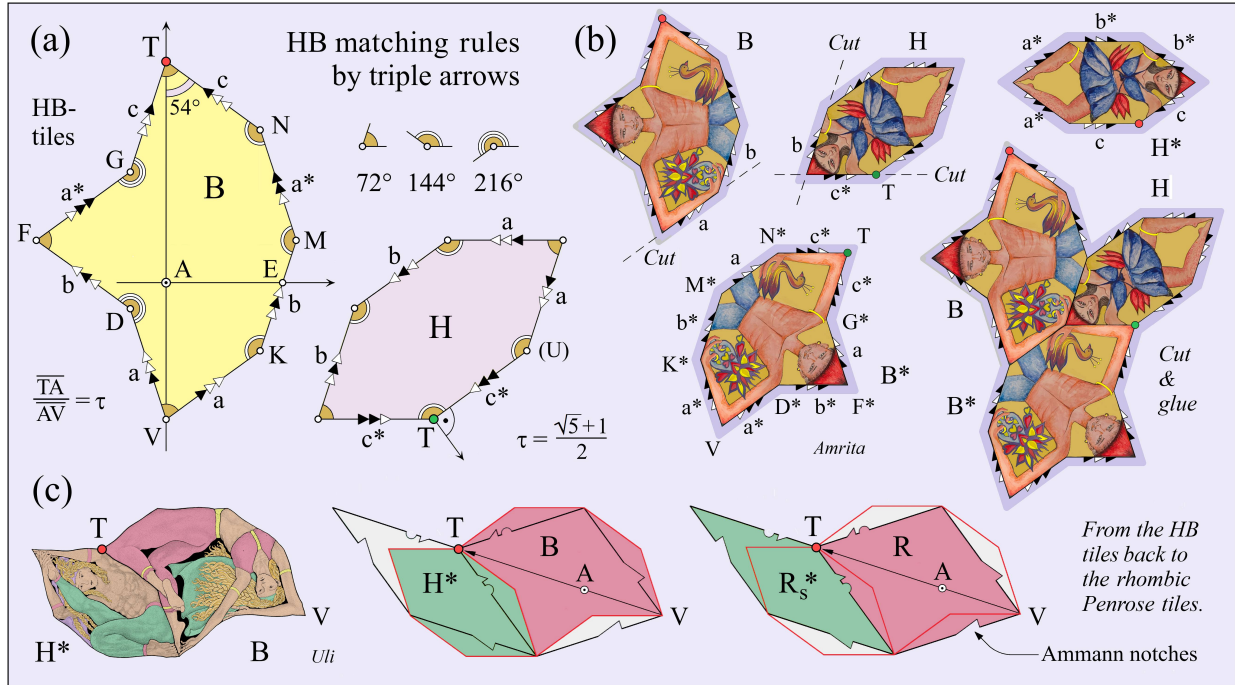


**Figure 2:** (a) *B* and *H* tile. (b) Artists with edge marks. (c) Re-conversion of *HB* tiles into rhombs.

In Figure 2(b), we propose a simple method for gluing tiles quasiperiodically together from paper copies. To do this, a border is left around the geometric tiles on which the outer half of the edge marks are drawn. The copies are then placed alongside each other so that identical marks are placed opposite. This is shown in Figure 2(b) on the left. One of the two opposite marks is then cut off along the dotted edge line. Now the three cut edges can be glued onto the uncut opposite borders, as shown on the right. To avoid *dead ends*, you should only glue tiles for which you have already designed a larger surrounding area!

### The Idea of an Algorithm for Designing Quasiperiodic *HB* Cartwheel Tilings

Since *Amrita* no longer had time to continue the project in its originally planned form, the author (*Uli*) preferred to continue the work by sketching an algorithm for a computer program in the complex plane  $\mathbb{C}$  that allows even inexperienced users to create artistic, quasiperiodic *HB* tessellations.

A cartwheel *C<sub>w</sub>4* with 180 tiles serves as a quasiperiodic framework for the algorithm. For clarity, we return to the Penrose rhombus tiling. Figure 2(c) shows the equivalence relation between the *HB* tiling and the rhombus tiling. The *Ammann notches*, which here define the matching rules, enforce mirror-image rhombs. Their indentations and protrusions correspond to the concave and convex angled edge pairs of the *HB* tiles. To avoid unnecessary detail, we will mark the edges in the following with the usual red Ammann line segments, even though the reflections of the rhombs are not visible in that way.

## Arithmetical Description of the Neighborhood Transformations $h$ in the Complex Plane $\mathbb{C}$

The basis for the description of a Penrose rhombus tiling are the ten *neighborhood transformations*  $h$  [8]. In Figure 3, only  $h_1$ ,  $h_2^*$ , and  $h_3$  are described in detail, as these can be considered as fundamental types. All ten valid neighborhood transformations prohibit periodic arrangements. In the following we calculate various, in some cases far-reaching transformations in the *complex plane*  $\mathbb{C}$ . The center of each rotation must be located at the origin  $O$  of the complex coordinate system!

The transformation  $h_1$  in Figure 3(a) is, geometrically seen, a counterclockwise  $72^\circ$  rotation of a copy of the purple rhombus  $R_{id}$  around its top point  $T$ . However, according to the cartwheel structure, we assign the point  $A_{id}$  of  $R_{id}$  to the origin  $O$ . The point  $A_{id}$  divides the long rhombus diagonal  $\overline{TV}$  of  $R_{id}$  in the golden ratio  $\tau : 1$ , with  $\tau = (\sqrt{5} + 1)/2$ . The index notation  $id$  of  $R_{id}$  refers to the *zero identity* of  $A_{id}$  at the origin  $O$ . The *transformation*  $h_1$ , described in  $\mathbb{C}$  as a rotation of  $R_{id}$  followed by a shift, generates one of the four *satellites* of the cartwheel  $Cw1$ . The rotation of the numbers  $z$  of the rhombus  $R_{id}$  with the angle  $\varphi_4$  is written as the complex product  $z \cdot w_4$  (The circular arrow  $\varphi_4$  shows the rotation of  $z_T$ ). The shift with the distance  $l$ , with  $l = \tau / \cos 18^\circ$ , is expressed by the addition of  $l \cdot v_2$ . The index 2 denotes that the shift direction of  $l$  (yellow arrow) forms an angle of  $36^\circ$  counterclockwise to the real axis  $Re$ .

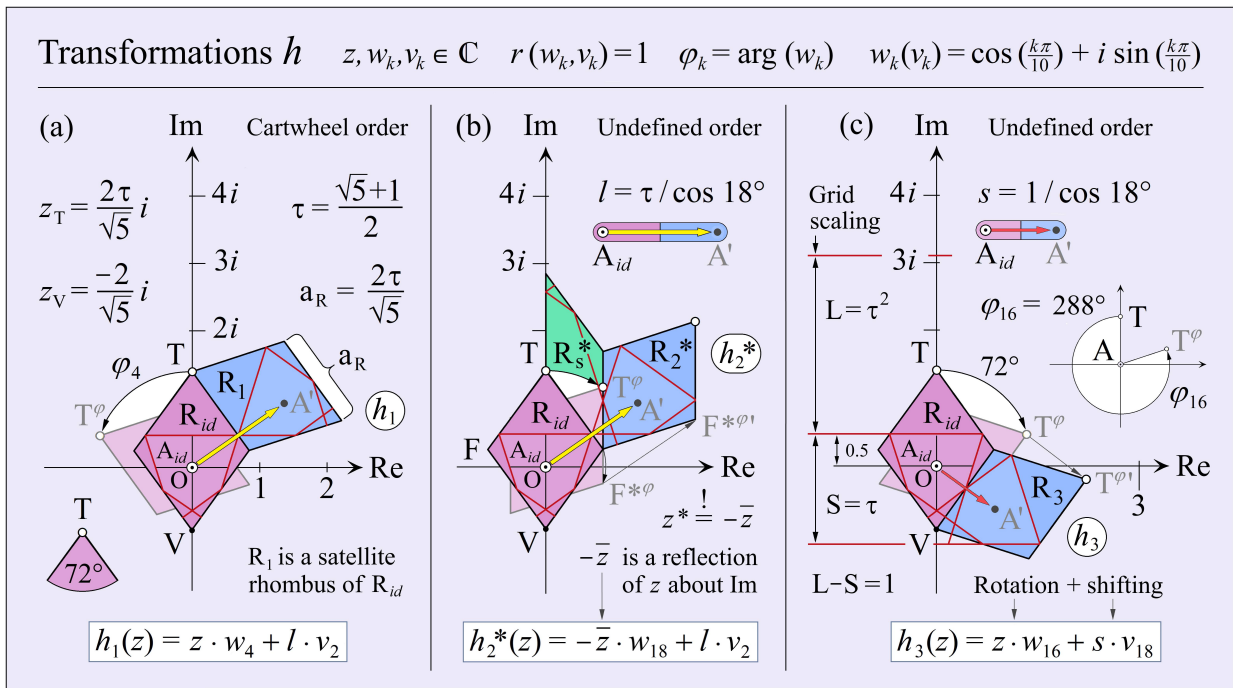


**Figure 3:** Three of the ten neighborhood transformations  $h$ : (a) Satellite rhombus  $h_1(R_{id})$ . (b)  $h_2^*$ . (c)  $h_3$ .

The transformation  $h_2^*$  in Figure 3(b) differs significantly from  $h_1$ , because the rotation angle is only  $36^\circ$ . The gap between the thick rhombs is filled with a green skinny rhombus  $R_s$  which has acute angles of  $36^\circ$ . At the positions of the points  $F$  and  $F^{*\varphi}$  can be seen that the rhombus  $R_{id}$  is first mirrored along its long diagonal before being rotated  $36^\circ$  clockwise. This is important for later use in the HB tiling. The shift of  $F^{*\varphi}$  to  $F^{*\varphi'}$  corresponds to an addition of  $l \cdot v_2$ . The result is the mirrored blue rhombus  $R_2^*$ .

The transformation  $h_3$  in Figure 3(c) is, geometrically seen, a clockwise  $72^\circ$  rotation over the point  $V$ . Expressed as a complex equation, the rotation is a multiplication of the numbers  $z$  and  $w_{16}$  ( $\varphi_{16} = 288^\circ$ ), i.e., the light purple rhombus in the background of  $R_{id}$  is rotated in the sense of the arrow  $72^\circ$  clockwise! The shift is the product of  $s$  and  $v_{18}$ , with  $s = 1/\cos 18^\circ$ . The direction is  $36^\circ$  clockwise to the real axis!

Only the position of the transformation  $h_1$  in Figure 3(a) corresponds to that one in a cartwheel  $Cw1$ , when this is centered as a basic *cluster* of seven rhombs in the origin of the complex plane  $\mathbb{C}$ .

## The Grid Basis of the Cartwheel $Cw4$ and its Hierarchical and Symmetric Structure

This version of the *quasiperiodic HB cartwheel algorithm* is limited to the size of the cartwheel  $Cw4$  in Figure 4, which is created by a *quasiperiodic Ammann grid* [2, 3, 4]. The eight *Ammann bars*  $L$  and  $S$  are generated by the substitution  $L_q \rightarrow LSLSL$  and  $S_q \rightarrow LSL$ . The sequence  $LSLSLLSL$  is called a *Fibonacci chain* or a *1D-Ammann grid*. The thickness of an  $L$  bar is  $\tau^2$  and that of an  $S$  bar is  $\tau$ . These grid values determine the basic scaling. Five 1D-grids are superimposed in five not symmetrical orientations! The result is a *5D-Ammann grid*, in which the Penrose rhombs can be clearly assigned to the grid meshes [2].

Before examining the overall structure of the cartwheel  $Cw4$ , we will first calculate the purple  $Cw1_{id}$  at the center of the complex plane  $\mathbb{C}$ , shown separately in the lower left. The equations of the four purple *satellite* rhombs are given on the left and right. The transformation  $h_1$  was already shown in Figure 3(a) as one of the four satellites. In the four satellite equations, the complex numbers  $z$  are defined as points of the central rhombus  $R_{id}$ . We use  $h_1, h_2, \dots$  [7] as a short index notation for  $h_1^{-1}, h_2^{-1}, \dots$  [8]!

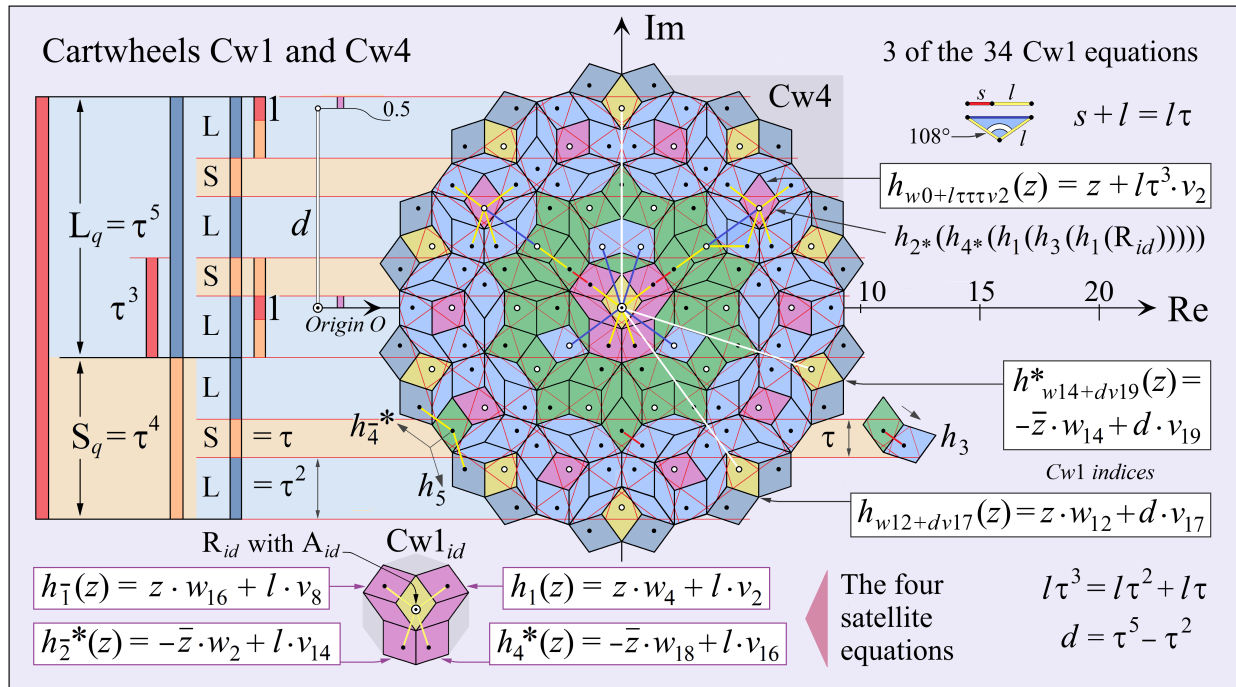


**Figure 4:** Left: Grid. Middle:  $Cw4$ . Bottom:  $Cw1_{id}$  with equations. Right: Full indexed  $Cw1$  equations.

Each rhombus  $R$  of a cartwheel  $Cw4$  could be described by a path of successively executed neighborhood transformations  $h$ , starting from  $R_{id}$  [7]. However, the  $Cw4$  cartwheel can also be created as a covering of 35 cartwheels  $Cw1$  (or  $Cw1^*$ ) whose centers  $A^\circ$  have only 20 distinct shift directions relative to the  $Cw4$  center  $A_{id}$ . Therefore, an algorithm for modular transformations seems to be an effective approach. From the equation  $l\tau^3 = l\tau^2 + l\tau$  we can deduce that the distance from the point  $A_{id}$  to the points  $A^\circ$  of the outer purple rhombs is equal  $l\tau^3$ , because two yellow shift lengths  $l$  with an internal  $108^\circ$  angle can be replaced by a (blue) length  $l\tau$ . The index notation of  $l\tau^3$  is  $l\tau\tau$ . The three  $Cw1$  equations on the right have the same form as the four satellite equations, except that  $z$  is defined here to be part of the overall  $Cw1_{id}$ .

The white points  $A^\circ$  of the ten outer purple rhombs are arranged in a regular decagon. The ten points  $A^\circ$  of the green rhombs also form a decagon, with the same directions from the origin, as well as the four points  $A^\circ$  of the four inner light blue rhombs. In these shifts with the shift lengths  $l\tau^3$ ,  $l\tau^2$ , and  $l\tau$  the index numbers  $k$  of  $v_k$  are even, where  $0 \leq k \leq 18$ . In contrast, the shift directions with the lengths  $d$  to the points  $A^\circ$  of the yellow rhombs, which are both decagonally arranged and regularly oriented, have  $v_k$  values with odd indices  $k$ , where  $1 \leq k \leq 19$ .

### Cw4 Sector with Overlapping HB Cartwheels Cw1 and their Complex Equations

Figure 5 shows a sector of the cartwheel Cw4 as an HB tiling, which can be seen in the lower left corner as a reduced rhombus version. Inside the sector, there are five B tiles and one B\* tile with a white point A°, each surrounded by four Cw1 satellites. The five B tiles are congruent to the B<sub>id</sub> tile without reflection, while the B\* tile and the cartwheel Cw1\* are mirror images of B<sub>id</sub> and Cw1<sub>id</sub>. The two Cw1\* satellites h<sub>2</sub>\*(B\*) and h<sub>4</sub>\*(B\*), located next to the white d line and marked with red circles, are mirrored twice. Since two reflections cancel each other out, these two satellites of B\* are unmirrored images of B<sub>id</sub>.

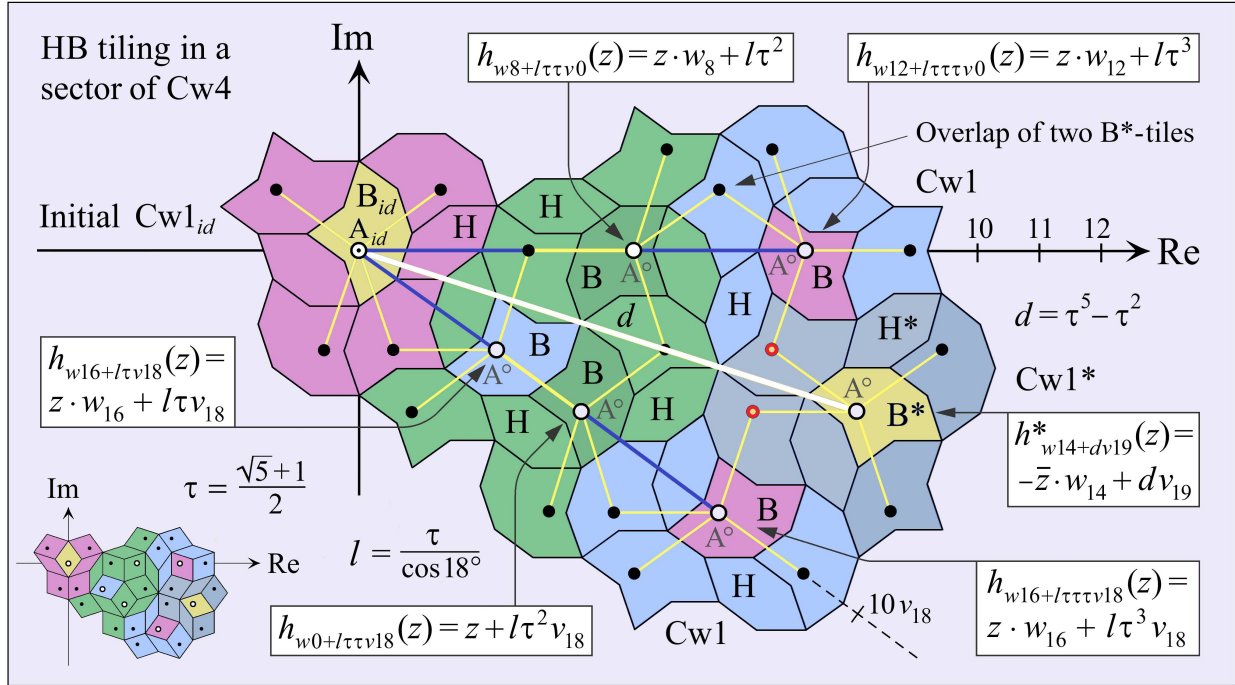


**Figure 5:** Seven overlapping HB cartwheels Cw1 with six Cw1 transformation  $h$  related to Cw1<sub>id</sub>.

The gapless covering of the 36° sector by the seven Cw1 cartwheels serves as an example of how the 35 Cw1 cartwheels cover the entire Cw4 area. The six transformations  $h$  of the initial purple cartwheel Cw1<sub>id</sub> are representative examples of the 34 Cw1 transformation equations. The sector is half divided by the white  $d$  line that leads from  $A_{id}$  to  $A^\circ$  of  $B^*$ . The three framed equations, that belong to the three  $B$  tiles below the  $d$  line, have the shift lengths  $l\tau$ ,  $l\tau^2$ , and  $l\tau^3$ , where the common shift direction is the boundary of the sector. Above the  $d$  line, the sector is delimited by the positive axis  $Re$ , with only two points  $A^\circ$  on it. In the two corresponding equations the number  $v_0$  ( $= 1$ ) is omitted because a factor 1 is unnecessary, just as  $w_0$  ( $= 1$ ) is omitted in the transformation  $h_{w_0+l\tau\tau v_{18}}$ . However, the numbers  $w_0$  and  $v_0$  are included in the indices to standardize them. Please note that we do not use indices within the indices!

With the standardized indices, the 34 Cw1 transformations can be easily applied to already computed results. As  $z$  is omitted in the indices, the mirroring transformations are identified by  $h^*$ , instead of  $-\bar{z}$ . Consequently, each index begins with the rotation number  $wk$ , followed by  $+d$  or  $+l$ , where  $l$  is always multiplied with  $\tau$ ,  $\tau\tau$ , or  $\tau\tau\tau$ . Finally, the shift direction is specified by a multiplication with  $vk$ .

### The Transformations of an Edge $e_{id}$ with Zero Identity to the Edges $a$ , $b$ , $a^*$ , and $c$ of $B_{id}$

It's our aim to assign three hand-drawn curved edges  $\alpha$ ,  $\beta$ , and  $\gamma$  to the marked edges  $a$ ,  $b$ ,  $a^*$ , and  $c$  of  $B_{id}$  and, in two further steps, to transform them onto the edges of the 115  $B$  tiles of Cw4. Therefore, we have first to define a zero identity of an edge  $e_{id}$  inside  $[A_{id}, E]$ , with  $A_{id}$  in the origin. Then we have to define the transformations of  $e_{id} \in \{a, b, c\}$  from  $[A_{id}, E]$  to the corresponding edge marks of  $B_{id}$ .



## The Construction of the Curved Edges and the Steps 1, 2, 3, and 4 of the Algorithm

Figure 7 shows that it is possible to substitute the straight edges  $a$ ,  $b$ , and  $c$  with curved edges, the *open Jordan curves* (without self-intersection)  $\alpha$ ,  $\beta$ , and  $\gamma$ . This substitution can have a figurative, ornamental, or geometric character. In the lower center of the image, a schematic Im-Re diagram shows how a freely drawn curved edge  $\alpha$  can be approximated by very short edge segments, which are generated successively by very small circles. The intersection of a circle with the curve  $\alpha$  generates the center point of the next circle. The created points, emphasized in black, can be understood as complex numbers  $z_\alpha$ . They can be projected vertically onto the real axis  $Re$ . There, marked as white dots, they represent the real part of the complex numbers  $z_\alpha$ . The rudimentary curve  $\alpha$  can be smoothed by circle segments or Bézier curves.

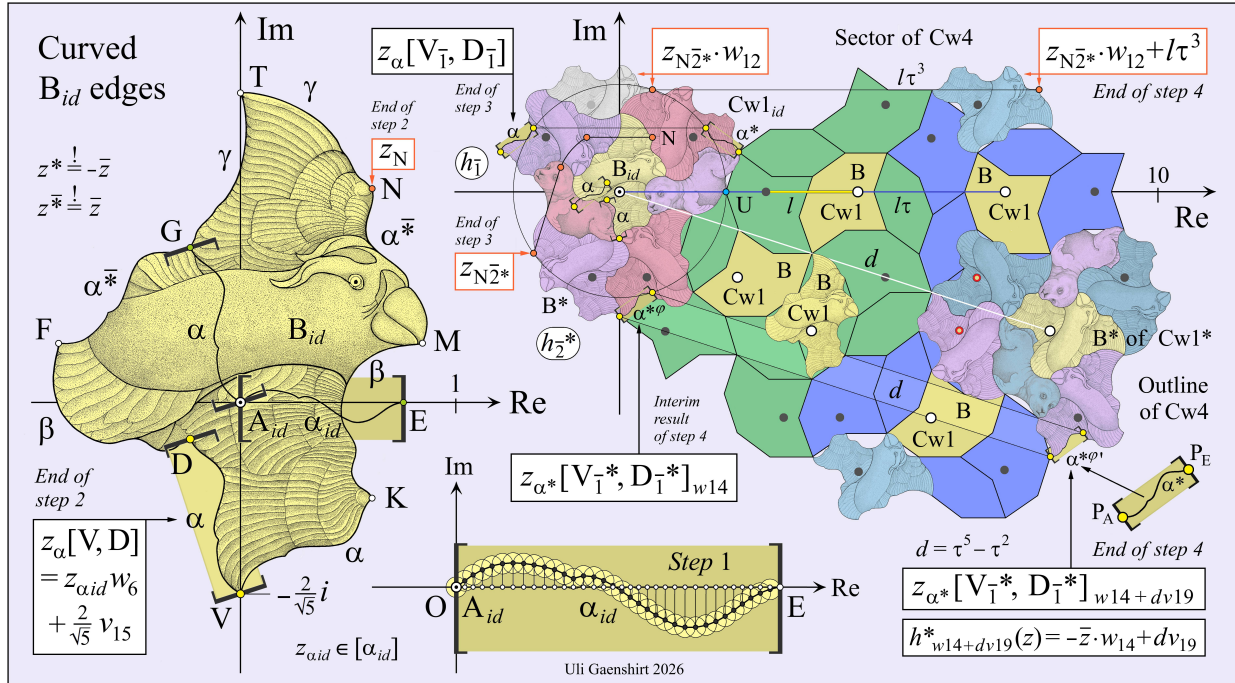


**Figure 7:** The four steps of the algorithm shown at the examples of figuratively designed tile edges.

The yellow bird on the left side of Figure 7 has exactly the same corner point geometry as the yellow  $B$  tile in Figure 6(a). There, we have already described the edge  $a_{id}$  as a set of points in the interval  $[A_{id}, E]$  in order to capture the properties of the edge marks. Therefore, the descriptions of the examples in step 2 in Figure 6(a) also apply here, whereby the curved edges are labeled  $\alpha$ ,  $\beta$ , and  $\gamma$ .

The two examples of step 3 in Figure 6(b) are shown in reduced size at the top middle of Figure 7. Therefore, only the start point  $N$  and the end point  $z_{N\bar{2}^*}$  of step 3 are named. The three edges  $a$  from step 3 in the green intervals in Figure 6(b) are curved edges here. They are simply marked with square brackets, and all three are labeled only with  $\alpha$ , so that the indexing can be used exclusively for step 4.

In step 4, the entire cartwheel  $Cw1_{id}$  is transformed. We use the equations as described in Figure 5. For the example of  $z_{N\bar{2}^*}$ , we choose the cartwheel  $Cw1$  on the far right part of  $Re$  as the final destination. We rotate  $z_{N\bar{2}^*}$  by multiplying it with  $w_{12}$ . The point  $z_{N\bar{2}^*} \cdot w_{12}$  belongs to the rotated bird in the background! Then we shift  $z_{N\bar{2}^*} \cdot w_{12}$  by  $l\tau^3$  parallel to the real axis  $Re$ . The result is the point  $z_{N\bar{2}^*} \cdot w_{12} + l\tau^3$ .

For the example of the curve  $\alpha$  with the point set  $z_\alpha[V_{\bar{1}}, D_{\bar{1}}]$ , we choose the only mirrored cartwheel  $Cw1^*$  in the sector of  $Cw4$ . So we first have to reflect  $\alpha$  about the  $Im$  axis and obtain  $\alpha^*$ . Then we rotate  $\alpha^*$  by a multiplication with  $w_{14}$  and receive  $\alpha^{*\phi}$  or, more precisely,  $z_{\alpha^*}[V_{\bar{1}}^*, D_{\bar{1}}^*]_{w_{14}}$ . Finally, we shift with  $dv_{19}$  and obtain  $\alpha^{*\phi'}$ , or, precisely, the set of the complex numbers  $z_{\alpha^*}[V_{\bar{1}}^*, D_{\bar{1}}^*]_{w_{14} + dv_{19}}$ .

## Summary

After an introduction to the geometry of the  $HB$  tiles and their practical application as puzzle pieces, the main part of the paper outlines an algorithm that makes it possible to digitally generate a quasiperiodic  $HB$  cartwheel  $Cw4$  using three self-designed curved edges, which are transformed by complex equations. In step 1, the edges are converted to point sets. In step 2, the curved edges are transformed onto the edges of the central  $B_{id}$  tile. In step 3, this  $B_{id}$  tile is transformed onto four satellite tiles of the cartwheel  $Cw1_{id}$ . In step 4,  $Cw1_{id}$  is transformed 34 times by complex equations to form the cartwheel  $Cw4$ .

## Conclusion and Outlook

The graphic artist M.C. Escher (1898–1972) was a globally renowned pioneer in the field of figurative periodic patterns [1]. Today, J. Richter-Gebert's computer program iOrnament enables users to design these periodic patterns with digital support [10]. A similar program for designing quasiperiodic tilings, as proposed in this paper, does not yet exist. The two representative examples, which guided you through the cartwheel algorithm in four steps each, show that this quasiperiodic algorithm can be used as the basis for a planned computer design program.

When designing the tiles, we must be aware that the lines often need to be redrawn, because if one of the edges is improved in relation to a specific part, four or six edges of this type within the two prototype tiles are changed at the same time. That is why designing quasiperiodic tilings promotes synergetic thinking. In this sense, the computer program would have enormous *educational potential* and would be perfectly suited for *interdisciplinary teaching*, without neglecting the fun factor.

The program should be available free of charge. It should be possible to draw the three curved edges (or more) with a pen on an external mobile phone or tablet, which can then be duplicated in the program and displayed on a screen. We will be very grateful for any help with programming, because we have no experience in this area. Support from an educational institution would be great.

## References

- [1] M.C. Escher. “The Official Website.” <https://mcescher.com>
- [2] U. Gaenshirt, A. Acharyya. “Reflected Motifs in Quasiperiodic Escher-Penrose Tilings.” *Proceedings of Bridges 2025: Mathematics and the Arts, 2025*, pp. 109–116. <https://archive.bridgesmathart.org/2025/bridges2025-109.html>
- [3] U. Gaenshirt. “Ammann Grid and Knot Structure of a Quasiperiodic Girih Pattern.” *Proceedings of Bridges 2024, 2024*, pp. 155–162. <https://archive.bridgesmathart.org/2024/bridges2024-155.html>
- [4] U. Gaenshirt. “Devilline's Talk.” *Bridges 2024 Conference Art Exhibition, 2024*. <https://gallery.bridgesmathart.org/exhibitions/bridges-2024-exhibition-of-mathematical-art/uli-gaenshirt>
- [5] U. Gaenshirt. “Quasicrystalline Wickerwork.” *Imaginary gallery*. <https://www.imaginary.org/gallery/quasicrystalline-wickerwork>
- [6] U. Gaenshirt. “Quasiperiodic Cartwheel Ballet.” *Bridges 2025 Conference Art Exhibition, 2025*. <https://gallery.bridgesmathart.org/exhibitions/bridges-2025-exhibition-of-mathematical-art/uli-gaenshirt>
- [7] U. Gaenshirt, M. Willsch. “The local controlled growth of a perfect Cartwheel-type tiling called the Quasiperiodic Succession.” *Philosophical Magazine*, vol. 87, 2007, pp. 3055–3065. <https://hal.science/hal-00513832>
- [8] P. Gummelt. “Penrose tilings as coverings of congruent decagons.” *Geom. Ded.*, 62, 1996, pp. 1–17.
- [9] R. Penrose. “Pentaplexity A Class of Non-Periodic Tilings.” *Math. Intell.*, Vol. 2, 1979, pp. 32–37.
- [10] J. Richter-Gebert. “Études in Symmetric Pattern Drawing.” *Proceedings of Bridges 2025: Mathematics and the Arts, 2025*, pp. 5–12. <https://archive.bridgesmathart.org/2025/bridges2025-5.html>